Original Article
DOI: https://doi.org/10.70749/ijbr.v3i9.2285

INDUS JOURNAL OF BIOSCIENCE RESEARCH
https://ijbr.com.pk
ISSN: 2960-2793/ 2960-2807

Crossref

OPEN ACCESS

Evaluation of Traditionally Used Medicinal Plants for Repurposing as Therapeutic Agents Targeting Human Diseases

Mustafa Kamal[1], Muhammad Junaid Yousaf[1], Basit Ali[1], Mughira Bin Zubair[2], Anwar Hussain[3], Aisha Siddique[4], Naveed Ali[3]

[1]Department of Botany, Government Post Graduate College Mardan, Pakistan
[2]Department of Botany, University of Peshawar, Peshawar, Pakistan
[3]Department of Botany, Abdul Wali Khan University Mardan, Pakistan
[4]Department of Microbiology, Women University Mardan, Pakistan

ARTICLE INFO

Keywords: Acetylcholinesterase, α-Glucosidase, Phytochemicals, Molecular docking, Donepezil, Neurodegenerative disorders.

Correspondence to: Muhammad Junaid Yousaf,
Department of Botany, Government Post Graduate College, Mardan, Pakistan.
Email: Junaidyousaf44@gmail.com

Declaration

Authors' Contribution: *Mentioned at the end of the paper.

Conflict of Interest: No conflict of interest.

Funding: No funding received by the authors.

Article History

Received: 24-06-2025 Revised: 26-08-2025
Accepted: 03-09-2025 Published: 15-09-2025

ABSTRACT

In silico drug design is a cost-effective method for identifying lead compounds before experimental validation. Owing to their lower toxicity and structural diversity, phytochemicals are increasingly being used as multitarget agents to treat complex disorders, such as diabetes and neurodegeneration. Using 70% ethanolic extracts, five traditionally medicinal plants including *Foeniculum vulgare, Trachyspermum ammi, Mentha piperita, Coriandrum sativum*, *and Cuminum cyminum* were investigated in this study. The identified phytochemicals through GC-MS analysis were molecularly docked using Schrödinger Maestro Version 2025-2. The binding affinities of acetylcholinesterase (AChE; PDB ID: 1eve) for neurodegeneration disorders and α-glucosidase (PDB ID: 3top) for diabetes were evaluated using donepezil and α-acarbose as reference inhibitors. The pharmacokinetics and toxicity profiles were estimated using the pkCSM platform. TMA24 exhibited the strongest affinity for AChE (docking score: −8.59 kcal/mol), outperforming donepezil (−7.91 kcal/mol) in the docking study. The enhanced binding was attributed to sulfur-mediated π–π stacking, hydrophobic interactions, and hydrogen bonding. TMA1 was the best-performing phytochemical (−6.42 kcal/mol), slightly lower than α-acarbose which had the highest interaction with α-glucosidase (−6.52 kcal/mol). The other compounds, PM3, TMA5, and PM10 also exhibited appreciated binding activities with the receptor proteins. According to the ADMET predictions, the phytochemicals exhibited superior intestinal absorption, CNS penetration, and Caco-2 permeability and have lower toxicity compared to the reference drugs. Therefore, the study highlighted that the reported druglike phytochemicals can act as the safer analogs against reference drugs such as donepezil and α-acarbose for the treatment of Alzheimer's and diabetic diseases, respectively. In-vitro and in-vivo validation and molecular dynamics simulations are to be incorporated into future studies to increase further specificity and safety.

INTRODUCTION

In silico techniques are a key part of contemporary drug discovery because they allow for the quick and economical screening of bioactive compounds against therapeutic targets (Zhang, Wu et al. 2022). Molecular docking, a popular computational method that offers information on binding affinity and possible biological activity, is used to predict a ligand's preferred orientation upon binding to a target protein (Akshaya, Dixit et al. 2025). Since medicinal plants provide a large library of structurally diverse natural compounds with potential pharmacological significance, the docking method is very beneficial for experiments of *in silico* drug designing (Ogbuagu, Mbata et al. 2022). *Foeniculum vulgare* (fennel), *Trachyspermum ammi* (ajwain), *Mentha piperita* (peppermint), *Coriandrum sativum* (coriander), and *Cuminum cyminum* (cumin) are widely used in traditional and modern medicine for their diverse therapeutic properties (Goyal, Chaturvedi et al. 2022, Zeeshan, Akram et al. 2023, Gupta, Kumar et al. 2024, Agarwal, Kanupriya et al. 2025). Fennel supports digestion, lactation, and respiratory health (Zafar, Khan et al. 2023); ajwain acts as a digestive aid with antimicrobial and bronchodilator effects (Singh, Yadav et al. 2021, Ullah, Hassan et al. 2024). peppermint, rich in menthol, alleviates nausea, bloating, and irritable bowel syndrome while providing cooling and analgesic actions (Kazemi, Iraji et al. 2025); coriander exhibits hypoglycemic, hepatoprotective, and detoxifying effects (Elbatawy, El-Mashad et al. 2025); and cumin improves digestion, regulates blood sugar, and lowers cholesterol (Garg 2023). Collectively, these plants serve as potent remedies for gastrointestinal, respiratory, inflammatory and various other metabolic disorders (Ansari, Reberio et al. 2025).

It is because they are rich in bioactive compounds such as flavonoids, alkaloids, terpenoids, phenolic acids, tannins, and essential oils (Dar, Shahnawaz et al. 2023). Flavonoids and phenolics function as antioxidants and anti-inflammatory agents, while alkaloids and terpenoids contribute to antimicrobial and spasmolytic activities (Bhatti, Ismail et al. 2022). Essential oils containing anethole, thymol, menthol, linalool, and cuminaldehyde provide strong therapeutic effects and interact with key biological targets, making these plants valuable leads in drug discovery (Mołdoch, Agacka-Mołdoch et al. 2025). Their natural structural diversity and pharmacological activities—such as enzyme inhibition, receptor modulation, and free radical scavenging (Rudrapal, Rakshit et al. 2024); offering the promising opportunities for developing novel drugs against chronic diseases including diabetes, cardiovascular disorders, microbial infections, neurodegenerative disorders and inflammation (Mohd Zaid, Sekar et al. 2023). These compounds have been linked to numerous therapeutic effects, even though their chemical mechanism of action is still unknown, particularly with regard to atomic-level interactions such as hydrogen bonds, ionic interactions, van der Waals forces, hydrophobic effects, π-interactions, and sometimes metal coordination or covalent binding between proteins and ligands (Yadav, Kaushik et al. 2022).

In order to better understand the therapeutic potential of these plants, this study looks at how their metabolic constituents interact with biologically significant protein targets that are connected to major human disorders (Trivedi, Shaikh et al. 2024). These medicinal plants may exert antidiabetic effects by inhibiting α-glucosidase (PDB ID: 3TOP), a key enzyme in carbohydrate digestion and postprandial glycemic regulation (Riyaphan, Pham et al. 2021). Inhibition of this enzyme delays the breakdown of complex carbohydrates into glucose, thereby reducing postprandial blood sugar spikes and improving overall glycemic control in diabetes management (Ayua, Nkhata et al. 2021). Similarly, acetylcholinesterase (AChE, PDB ID: 1EVE), the enzyme responsible for breaking down acetylcholine in the brain, is a validated therapeutic target in Alzheimer's disease (Suha, Hossain et al. 2025), as its inhibition can enhance cholinergic transmission and improve cognitive function (Subramaniam, Blake et al. 2021).

The aim of this study is to find the possible lead compounds of the traditional medicinal plants such as Fennel, Ajwain, Peppermint, Coriander, Cumin for mechanistic interactions to treat diabetes and neurogenerative disorders by analyzing docking conformations, binding affinities, and interaction patterns of metabolites detected with 3top and 1eve receptor proteins. This will help the future in-vitro and in-vivo research, which would encourage the sensible creation of drugs derived from plants (Najmi, Javed et al. 2022).

MATERIALS AND METHODS

Preparation of Ethanolic Extract

The fresh leaves of medicinal plants from five selected species, *F. vulgare, T. ammi, M. piperita, C. sativum***,** *and C. cyminum* were collected from the Mardan division of Khyber Pakhtunkhwa. These materials were carefully washed in sterilized distilled water so as to remove debris and then shade dried in room temperature (25 ± 2 °C) over 15 days under sterilized conditions (Mishra, Dash et al. 2024). The samples dried were then reduced to fine powder using mechanical grinder and sifted through a sieve with a 40-mesh to eliminate large particles (Bhujle, Nayak et al. 2025). To extract, 50 g of each powdered plant was added in a 250 mL ethanol (70% in water v/v) amber glass container and shaken intermittently throughout 14 days in the amber glass container at room temperature (Bharath 2023). Whatman No. 1 filter paper was used to filter the mixture, and the filtration was concentrated by evaporating ethanol using a rotary evaporator under the following conditions: 40 °C water bath temperature, 120 mbar vacuum pressure, 110 rpm rotation speed, and 10 °C condenser temperature (Andze, Vitolina et al. 2024). Semi-solid extracts formed were further dried in a desiccator to remove the remaining solvent and kept in airtight containers at 4 °C for pending analysis.

Determination of Antioxidant Potential

The 2,2-diphenyl-1-picrylhydrazyl (DPPH) free radical scavenging assay was utilized for the determination of antioxidant potential of the selected plant samples (Tatarczak-Michalewska and Flieger 2022) . Initially, the 1 mL of fresh stock solution of DPPH (0.01 mM; 3.94 mg of DPPH dissolved in 100 mL methanol) was added to the 1 mL of extract sample and kept for incubation in the dark for 30 min at room temperature. The decrease in absorbance was measured at 517 nm using a UV–visible spectrophotometer. The percentage of radical scavenging activity was calculated by comparing the absorbance of the sample with that of the control, and the concentration required to inhibit 50% of the radicals (IC_{50}) was determined. Lower IC_{50} values indicate higher antioxidant activity.

Gas Chromatography–Mass Spectrometry (GC-MS) analysis

GC-MS analysis was performed using the established protocols (Chanu, Chanu et al. 2024, Endris, Abdu et al. 2024). Briefly, the dried ethanolic extracts were reconstituted in HPLC-grade methanol (1.0 mg/mL), vortex-mixed (2 min), sonicated (10 min) and filtered using 0.22 µm PTFE syringe filters. In the case of non-volatile/thermolabile constituents, an aliquot (200 µL) was evaporated under a N_2 atmosphere followed by derivatization with N-Methyl-N-trimethylsilyl trifluoroacetamide (MSTFA) (200 µL; 60 °C, 30 min). GC-MS was conducted on a capillary column with EI source (70 eV) and low-polarity column (HP-5MS or DB-5ms, 30 m x 0.25 mm i.d, 0.25 u m film thickness). Helium gas was used as the carrier gas at constant flow. Samples (1 µL) were injected under split mode (10:1) at 250 °C with solvent delay time of 3.0 min. The oven was set as follows: 60 °C (2 min), ramp 10 °C /min to 300 °C, hold 10 min (reaction period of about 32 min in total). The parameters of the MS were as follows, transfer line, 280 °C; ion source, 230 °C; quadrupole, 150 °C; scan range, m/z 40-550; scan rate, 3.0 scans/s. A homologous series of n-alkanes (C8-C40) were measured under the same condition to calculate the Kovats/linear retention indices. Mass-spectral library matching (e.g., NIST/Wiley; match ≥ 80) with retention indices (± 20 RI units). The values of the TIC peaks were normalized by the area of baseline-corrected deconvolution TIC peaks to give their relative abundances. All extracts were subjected to three analytical observations to determine the technical variation (RSD%). Data collection and analysis were done via vendor software (e.g., MassHunter/Xcalibur) and the reports contained retention time, RI, base ions, library match scores, and percentage peak area. The metabolites detected from *F. vulgare* was denoted by FV, *T. ammi* was denoted by TMA, *M. piperita* was denoted by PM, *C. sativum* was denoted by CS, and *C. cyminum* was denoted by CC.

Ligand Preparation

All chemical compounds selected for molecular docking were initially sourced from publicly available chemical databases such as PubChem (https://pubchem.ncbi.nlm.nih.gov) or ZINC20 (https://zinc.docking. org) databases (Marbán-González, Ramírez-Cid et al. 2025). To validate structures of the ligands, ChemDraw Ultra (Version 2022) and Open Babel (version 3.1.1) were utilized after they were downloaded in SDF format from PubChem or ZINC20 databases (Thakur, Gupta et al. 2025). The most stable conformer was then found by energy minimization using the MMFF94 force field after the two-dimensional chemical structures were converted into three-dimensional conformations (Xie, Wang et al. 2022). Invalid stereoisomers, unnecessary tautomer, and duplicate entries were removed, and the shape of each ligand was monitored (Zhang, Vass et al. 2023). Proper ionization was achieved by setting protonation states to physiological pH (~7.4) (Gaohua, Miao et al. 2021). Schrödinger's LigPrep module (for Glide docking) were used for additional energy optimization and ligand structure cleanup in compliance with the requirements of each docking experiments (Bathula, Muddagoni et al. 2021).

Determination of Physicochemical Descriptors

The physicochemical properties of the compounds were calculated using RDKit version 2023.09.1 in Python (Ayres, Bandara et al. 2024). SMILES representations of all molecules were first converted into RDKit molecular objects, which were then used to compute key descriptors relevant for drug design, including molecular weight, LogP (octanol–water partition coefficient), topological polar surface area (TPSA), number of hydrogen bond donors and acceptors, and rotatable bonds and PAINS alert using machine learning model (fpscores.pkl). These descriptors provide insights into the compounds' drug-likeness, and bioavailability (Roba and Umar 2025).

Protein Preparation

The target proteins of three-dimensional crystal structures (PDB ID: 3top and 1eve) were obtained from the RCSB Protein Data Bank (RCSB PDB) (https://www.rcsb.org/) (Agnihotry, Pathak et al. 2022). Structures with the low resolution and co-crystallized ligands were prioritized (Li, Li et al. 2024). The proteins were first examined using UCSF Chimera 1.19.0 for missing loops (Mitra, Kumar et al. 2025). When missing loops or incomplete residues were observed, MODELLER was utilized for modeling and structure refinement (Studer, Tauriello et al. 2021). Ultimately, the final structure underwent an energy reduction process using Swiss-PDB Viewer (Version 4.1) prior to grid generation or binding site definition (Owoloye, Ligali et al. 2022).

Molecular Docking with Schrödinger Glide

The structure-based docking was done using the Maestro interface of Schrödinger's Glide module (Schrödinger Release 2025-2) (Roy, Sharma et al. 2024). The protein structures were reassessed for removal of water molecules that were more than 5 Å from the active site, addition of missing hydrogen atoms, correction of bond ordering, and energy reduction using the OPLS4 force field. All of these were done using the Protein Preparation Wizard. To construct a receptor grid, the centroid of the co-crystallized ligands was utilized. To increase precision, promising hits were re-docked in Extra Precision (XP) mode after the initial docking was done in Standard Precision (SP) mode.

ADMET Property Prediction

The pkCSM web server (http://biosig.unimelb.edu.au/pkcsm/) was used to predict pharmacokinetics and toxicity predictions (Adnyaswari, Wiwiek Indrayani et al. 2024). Each ligand was subulate to predict key Absorption, Metabolism, Excretion, Toxicity (ADMET) parameters, such as absorption (Caco-2 permeability, intestinal absorption, and P-glycoprotein substrate/inhibition), distribution (volume of distribution, blood brain barrier permeability), metabolism (cytochrome p450 interactivity, including CYP3A4 and CYP2D6), excretion (total clearance), and toxicity profiles (AMES mutagenicity, hepatotoxicity, skin sensitization, hERG inhibition, and LD_0). Furthermore, the similarity to drugs was investigated according to such standard guidelines as the Rule of Five by Lipinski and the criteria developed by Veber.

RESULTS AND DISCUSSION

Determination of Antioxidant Activity

The antioxidant activities of ethanolic extracts from *F. vulgare*, *T. ammi*, *M. piperita*, *C. sativum*, and *C. cyminum* were evaluated using the DPPH free radical scavenging assay. The IC_{50} values are presented in Figure 1. Among the tested plants, *T. ammi* exhibited the strongest antioxidant activity with an IC_{50} of 0.43 ± 0.03 µg/mL (a), indicating a high free radical scavenging potential. *C. cyminum* and *F. vulgare* also showed substantial activity with IC_{50} values of 0.45 ± 0.06 µg/mL (b) and 0.57 ± 0.05 µg/mL (c), respectively. In contrast, *M. piperita* and *C. sativum* displayed comparatively weaker antioxidant activity, with IC_{50} values of 0.80 ± 0.04 µg/mL (d) and 0.70 ± 0.04 µg/mL (d), respectively.

All the IC_{50} values observed in this study are well below the commonly accepted threshold of 1 µg/mL for strong antioxidant activity, indicating that all tested extracts exhibit significant radical scavenging potential suitable for pharmaceutical and nutraceutical applications. The variation in antioxidant activity among these species can be attributed to differences in their phytochemical composition, particularly the content of phenolic compounds, flavonoids, and essential oil constituents (Guedri Mkaddem, Zrig et al. 2022). The higher activity of *T. ammi* and *C. cyminum* may be due to the presence of bioactive compounds such as thymol, anethole, and cuminaldehyde, which are known for their strong radical scavenging properties (Modareskia, Fattahi et al. 2022, Mughal 2022). *F. vulgare* also demonstrated notable antioxidant effects, likely due to anethole (Barakat, Alkabeer et al. 2022). On the other hand, the relatively weaker activity observed in *M. piperita* and *C. sativum* may reflect lower concentrations of potent phenolic antioxidants such as menthol, Rosmarinic acid, or other flavonoids (Hudz, Kobylinska et al. 2023, Lahlou, Bounechada et al. 2025). Overall, these results suggest that all selected plants possessed promising antioxidant potential and could be utilized as natural sources of antioxidants in food and pharmaceutical applications.

Figure 1

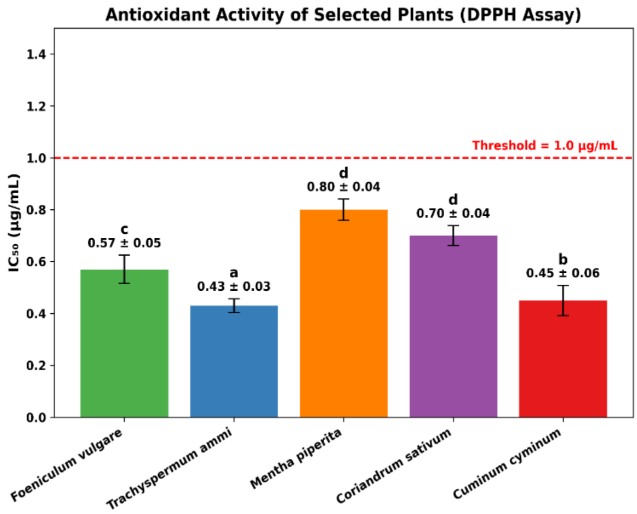

This figure illustrates the antioxidant activity (DPPH assay) of selected medicinal plants, expressed as IC_{50} values (µg/mL). All tested extracts exhibit strong radical scavenging activity below the threshold of 1.0 µg/mL. Among them, Trachyspermum ammi (0.43 ± 0.03 µg/mL) and Cuminum cyminum (0.45 ± 0.06 µg/mL) show the most potent activity, followed by Foeniculum vulgare (0.57 ± 0.05 µg/mL). *Coriandrum sativum* (0.70 ± 0.04 µg/mL) and Mentha piperita (0.80 ± 0.04 µg/mL) also demonstrate significant but comparatively lower activity. Different letters above bars indicate statistically significant differences ($p < 0.05$).

Screening of druglike compounds

The 70% ethanolic extracts of five selected medicinal plants *F. vulgare, T. ammi, M. piperita, C. sativum, and C. cyminum* were subjected to the GC-MS analysis (Figure 2A-2E), which detected a total number of 118 phytochemical compounds (Supplementary Data S1). These compounds were subsequently assessed in terms of drug-likeness according to the five rules of Lipinski and the rule of Veber. Lipinski rule means that any compound with a molecular weight of 500 Da or lower, a logP of 5 or less, 5 or fewer hydrogen bond donors and 10 or fewer hydrogen bond acceptors (Nhlapho, Nyathi et al. 2024) and the Veber's rule through rotatable bonds ≤10 and topological polar surface area (TPSA) ≤140 Å ensures good oral bioavailability (Möbitz 2024). These rules play an important role in the development of drug design by identifying the potential chemical compounds extracted from plants by eliminating the compounds with poor chances of absorption or bioavailability (Lohit, Singh et al. 2024). According to these criteria, 96 compounds were found that met both Lipinski and Veber rules (Figure 3A). The druglike compounds comprised of 25 compounds in *T. ammi*, 29 compounds in *F. vulgare*, 14 compounds in *M. piperita*, 13 compounds in *C. sativum* and 15 compounds in *C. cyminum* (Figure 3B).

To evaluate the interdependence of the physicochemical descriptors of these 96 compounds, pairwise correlation analysis was performed using scatter plots with regression fitting (Figure 4) and a correlation heatmap (Figure 5). The scatter plots revealed several strong linear relationships among the descriptors. Molecular weight showed a high positive correlation with lipophilicity (LogP; R^2 = 0.88) and rotatable bonds (R^2 = 0.81), and a strong negative correlation with hydrogen bond donors (R^2 = -0.92) and acceptors (R^2 = -0.71). Hydrogen bond donors correlated strongly with acceptors (R^2 = 0.89) and inversely with rotatable bonds (R^2 = -0.97). TPSA exhibited moderate positive correlation with hydrogen bond acceptors (R^2 = 0.72) but minimal association with LogP (R^2 = 0.01), indicating the relative independence of polarity from lipophilicity in this compound set.

The correlation heatmap (Figure 5) further confirmed these findings. Molecular weight showed the highest positive correlation with LogP (r = 0.94) and rotatable bonds (r = 0.90), and a strong negative correlation with hydrogen bond donors (r = –0.96). Hydrogen bond donors were strongly inversely correlated with rotatable bonds (r = –0.98) and acceptors (r = –0.94). In contrast, TPSA displayed weaker correlations with most descriptors, except for a moderate positive association with hydrogen bond acceptors (r = 0.85). Overall, these results highlight clear interdependencies among descriptors relevant to Lipinski's and Veber's rules. The strong associations between molecular weight, LogP, rotatable bonds, and hydrogen bonding features suggest that optimization of one parameter could significantly influence others. TPSA, however, emerged as an independent descriptor, providing complementary information on polarity and molecular surface properties.

A

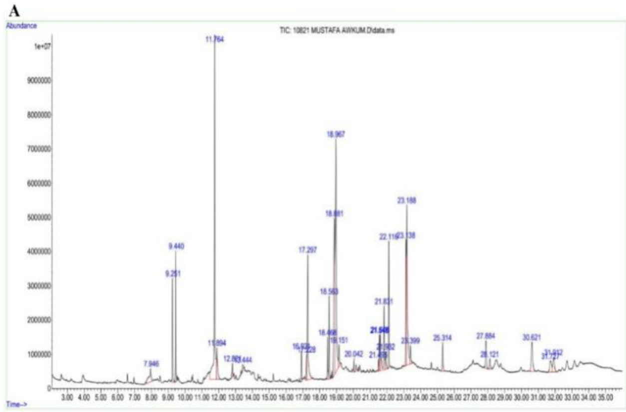

B

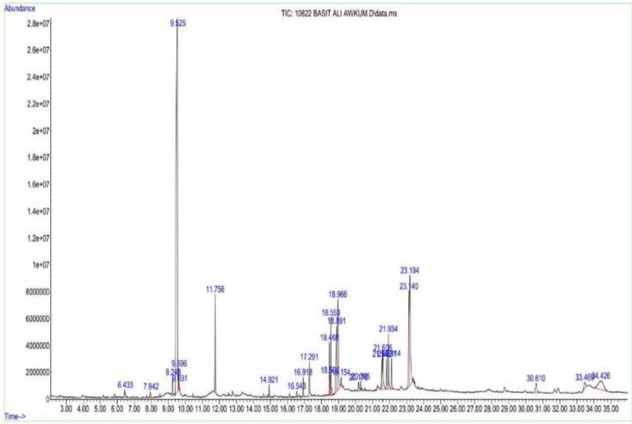

C

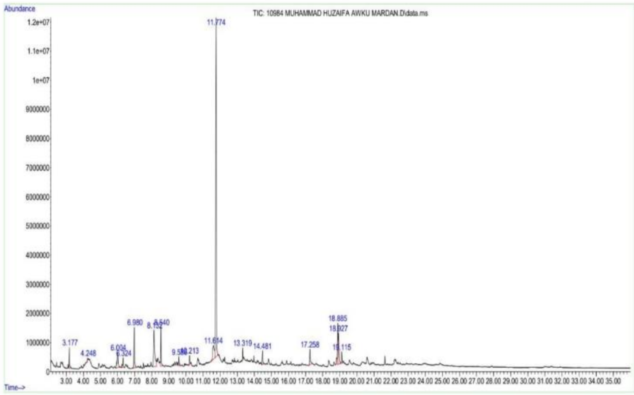

D

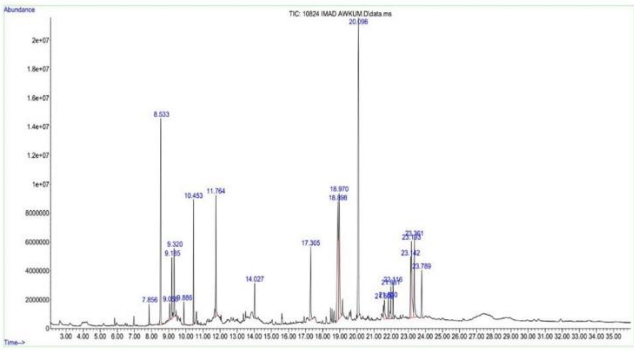

E

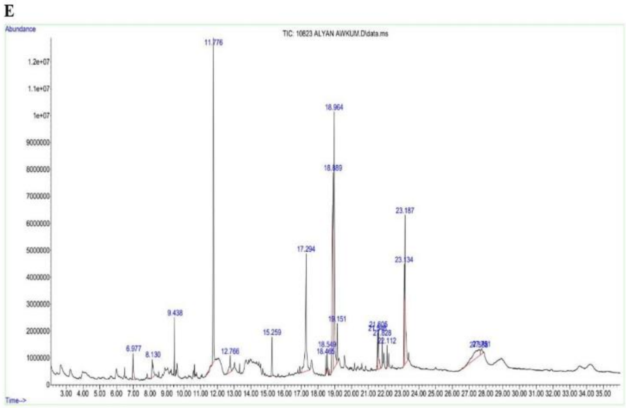

GC-MS Chromatograms of A (*Foeniculum vulgare*), B (*Trachyspermum ammi*), C (*Mentha piperita*), D (*Cuminum cyminum*), E (*Coriandrum sativum)* of 70% ethanolic extract shows the detection of compounds used for drug designing.

Figure 3

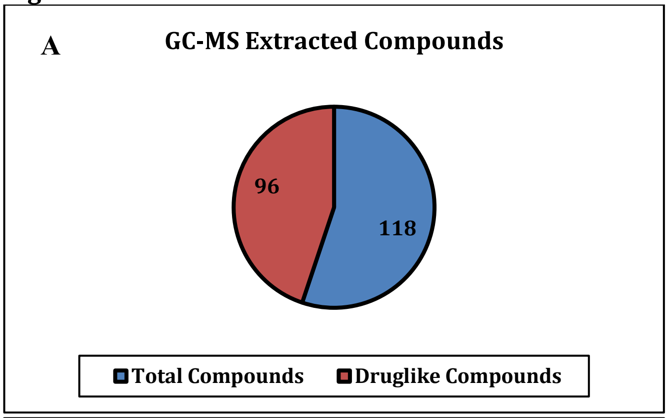

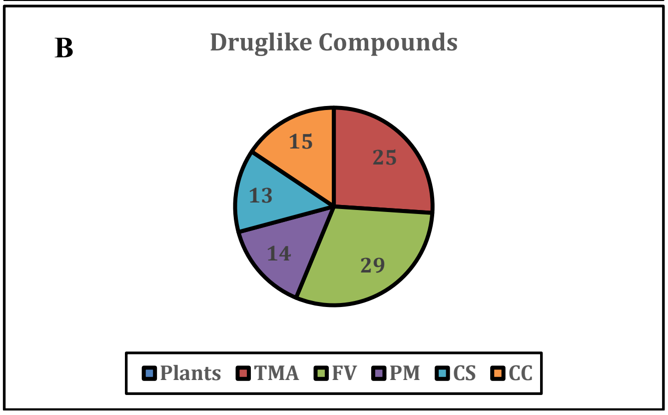

Figure 3A show the GC–MS analysis of five medicinal plants identified 118 compounds, among which 96 were drug-like based on Lipinski and Veber criteria, and Figure 3B shows their distribution across the plants is shown such as TMA (*Trachyspermum ammi*), FV (*Foeniculum vulgare*), PM (*Mentha piperita*), CS (*Coriandrum sativum*), CC (*Cuminum cyminum*).

Figure 4

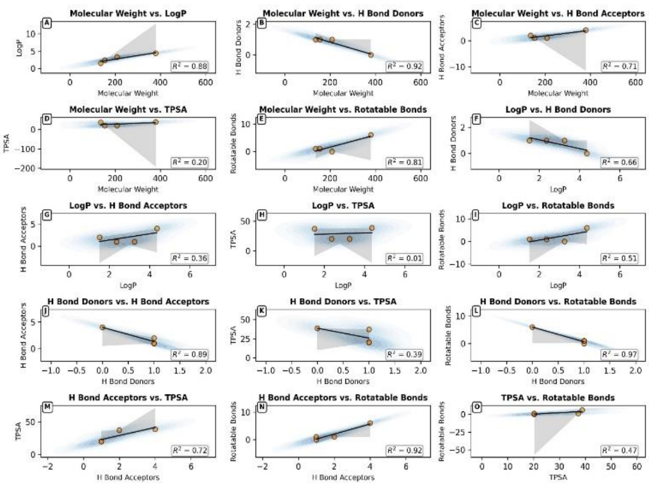

This figure presents pairwise correlation plots between key molecular descriptors: molecular weight (MW), LogP, hydrogen bond donors (HBD), hydrogen bond acceptors (HBA), topological polar surface area (TPSA), and rotatable bonds (RB). Each subplot (A–O) shows scatter points with regression lines, 95% confidence intervals, and the corresponding coefficient of determination (R^2). Strong correlations are observed for MW vs. HBD, HBD vs. RB, HBA vs. TPSA, and HBA vs. RB, while weak or negligible correlations appear for LogP vs. TPSA and MW vs. TPSA.

These relationships highlight the interdependence of drug-likeness descriptors commonly applied in medicinal chemistry.

Figure 5

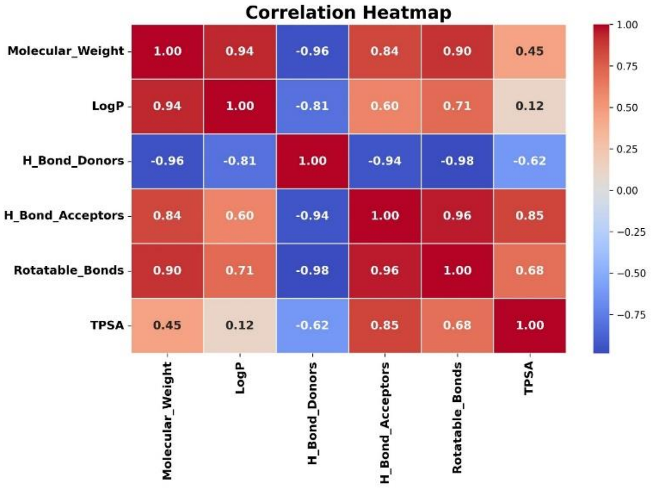

This heatmap shows the pairwise correlation coefficients between molecular descriptors: molecular weight (MW), LogP, hydrogen bond donors (HBD), hydrogen bond acceptors (HBA), rotatable bonds (RB), and topological polar surface area (TPSA). Strong positive correlations are observed between MW, HBA, and RB ($r > 0.84$), while HBD is strongly negatively correlated with these descriptors ($r < -0.94$). TPSA correlates positively with HBA ($r = 0.85$) and moderately with RB ($r = 0.68$) but shows weak or negligible correlation with MW and LogP. These trends highlight descriptor interdependencies, where molecular size and flexibility often increase with acceptor count, while donor count inversely relates to these properties.

Molecular Docking Using Schrodinger Maestro

The molecular docking simulation used to assess the binding affinity of the screened phytochemicals with the acetylcholinesterase (PDB ID: 1eve) and alpha-glucosidase (PDB ID: 3top) were performed using donepezil and alpha-acarbose as standard inhibitors, respectively. Inhibition of 3top proteins delays the breakdown of complex carbohydrates into glucose, thereby reducing postprandial blood sugar spikes and improving overall glycemic control in diabetes management (Ayua, Nkhata et al. 2021). Similarly, acetylcholinesterase (AChE, PDB ID: 1EVE), the enzyme responsible for breaking down acetylcholine in the brain, is a validated therapeutic target in Alzheimer's disease (Suha, Hossain et al. 2025), as its inhibition can enhance cholinergic transmission and improve cognitive function (Subramaniam, Blake et al. 2021).

Molecular docking using Schrodinger demonstrated that TMA24 had a higher binding affinity to acetylcholinesterase than donepezil (-7.91 and -58.69 kcal/mol), docking score: -8.59 kcal/mol and Glide energy: -56.12 kcal/mol. This enhanced performance can be credited to the sulfur substituents in TMA24 that enhance π–π stacking and hydrophobic interactions with aromatic residues of 1eve receptor proteins. Its -0.32 contribution to hydrogen bonds and lipophilicity (glide_lipo = -4.57) imply that it has more stabilizing interactions within the binding pocket whereas the Glide Gscore of -10.81 suggests that donepezil is extremely compatible with the active site. The larger docking score of TMA24 suggests that structural diversity among phytochemicals can result in superior inhibitory potential (Figure 6).

There was a moderate binding of acetylcholinesterase to the other ligands. TMA5 used hydrophobic contacts with minimal hydrogen bonding and thus docking had a score of -7.77 kcal/mol. This was likely due to its bulk structure that did not allow the best fit. PM3 exhibited positive stability with π -π stacking interactions, van der Waals interactions, and minimal hydrogen bonding (-7.52 kcal/mol). TMA19 exhibited good lipophilic interactions as it could achieve a score of -7.43 kcal/mol. The binding potential of PM10 was much less but still notable as indicated in the docking score -7.28 kcal/mol. These findings suggest that the hydrophobicity and aromaticity of these ligands play an important role in stabilization of the enzyme active site of acetylcholinesterase (Figure 6).

The most affine reference inhibitor was α-acarbose, with docking score of -6.52 kcal/mol and glide energy of -61.70 kcal/mol due to strong hydrogen bonding (-0.34) by its carbohydrate-like structure. TMA1 had the closest docking score of -6.42 kcal/mol to α-acarbose. TMA1 exhibited significant lipophilic interactions (0.79) and slight hydrogen bonding (0.44), which meant that it stabilized by both polar and hydrophobic interactions. The next was PM3 with a docking score of -6.36 kcal/mol. Despite exhibiting minimal hydrogen bonding, it has a favorable binding energy of -40.78 kcal/mol, indicating that van der Waals interactions and π–π stacking dominate the binding process. PM10 and TMA5 docking scores were -6.20 kcal/mol and -6.05 kcal/mol respectively, indicating that these compounds were predominantly stabilized mainly through hydrophobic interactions rather than hydrogen bonding (Figure 7).

In general, these results point to two different forms of inhibitory strategy: hydrophobic/aromatic-driven, which is notable with TMA24, PM3, and TMA5, and hydrogen-bond-driven, which is notable with alpha-acarbose and TMA1. TMA1 and PM3 were highly promising with regards to anti-alpha-glucosidase, and TMA24 the best candidate with regards to anti- acetylcholinesterase. The 2D structure of these complexes were visualized in Figure 8 and the druglike properties as described in Veber rule and Lipinski rule were visualized in Figure 9.

Figure 6

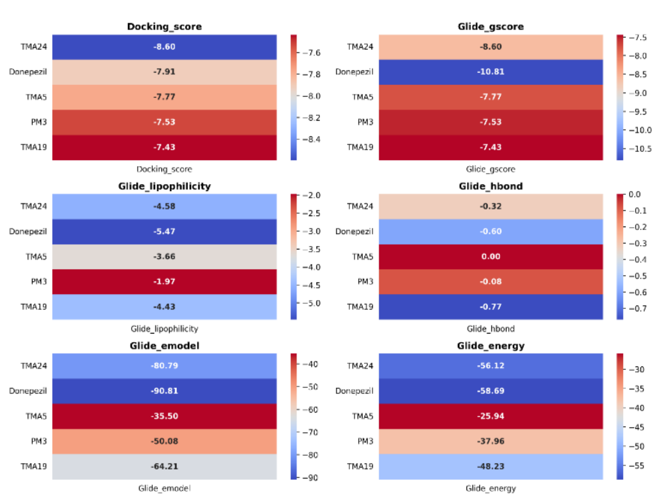

Figure shows the 1eve docking results of test ligands (TMA24, TMA5, TMA19, PM3) compared with the reference drug Donepezil across six parameters: docking score, Glide gscore, lipophilicity, hydrogen bonding, emodel, and energy. Donepezil demonstrates the strongest overall binding affinity and stability, particularly with the lowest Glide gscore (−10.81) and most favorable emodel (−90.81). Among the test compounds, TMA24 stands out with a competitive docking score (−8.60), favorable energy values, and stable interaction potential, making it the most promising candidate.

Figure 7

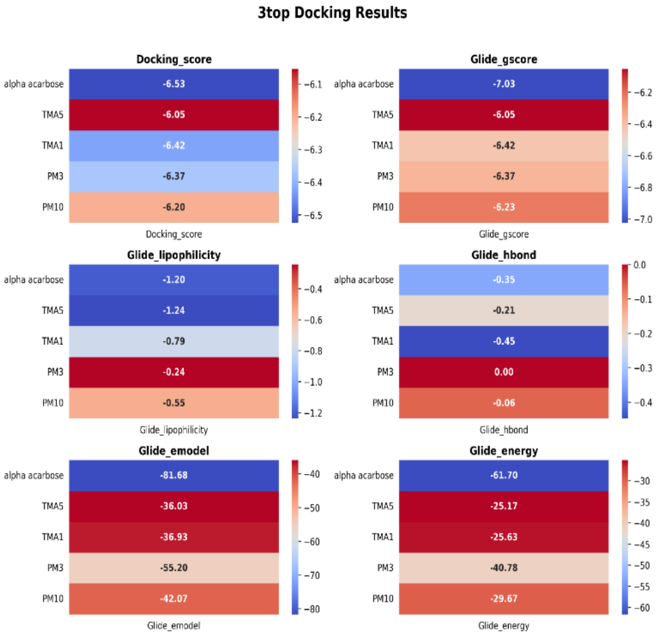

Figure shows the 3top docking results of test ligands (TMA5, TMA1, PM3, PM10) compared with the reference inhibitor α-acarbose across six parameters: docking score, Glide gscore, lipophilicity, hydrogen bonding, emodel, and energy. α-Acarbose demonstrates the most favorable overall binding (Glide gscore −7.03; emodel −81.68; energy −61.70). Among the test ligands, TMA1 and TMA5 display competitive docking and gscore values, while PM3 shows stronger lipophilic contributions. Overall, α-acarbose remains the strongest binder, but TMA1 and TMA5 emerge as promising candidates with potential stability and interaction efficiency.

Figure 8

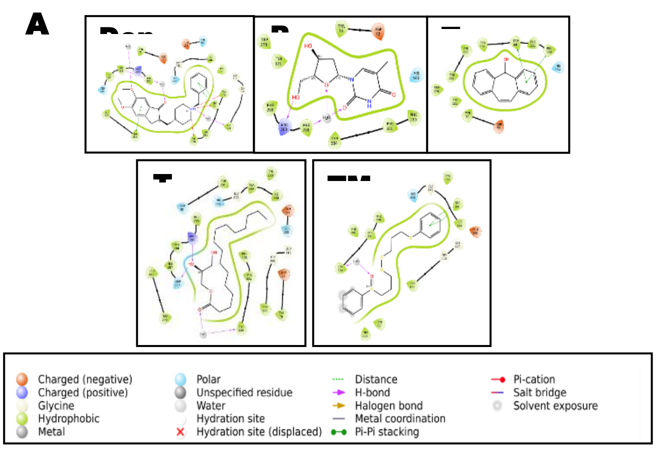

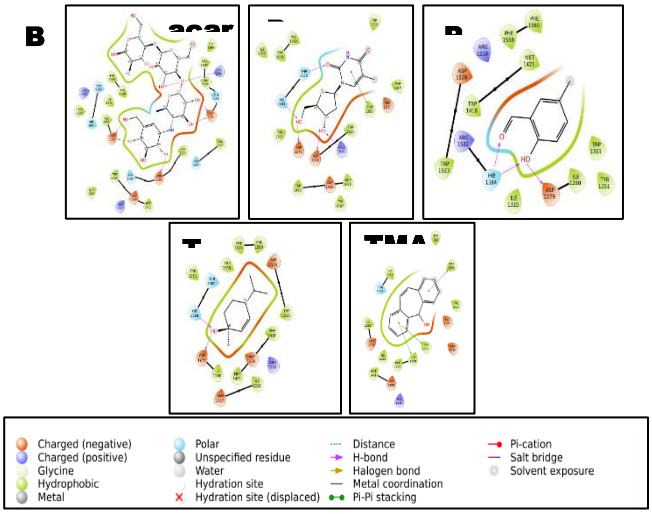

The figure presents the comparative interaction patterns of Donepezil (A) and Acarbose (B) with selected molecular targets. Donepezil exhibits strong associations with TMA5, PM3, TMA19, and TMA24, whereas Acarbose interacts predominantly with PM3, PM10, TMA1, and TMA5. These distinct profiles emphasize differences in the binding specificities of the two compounds, suggesting possible mechanistic divergence in their biological activities.

Figure 9

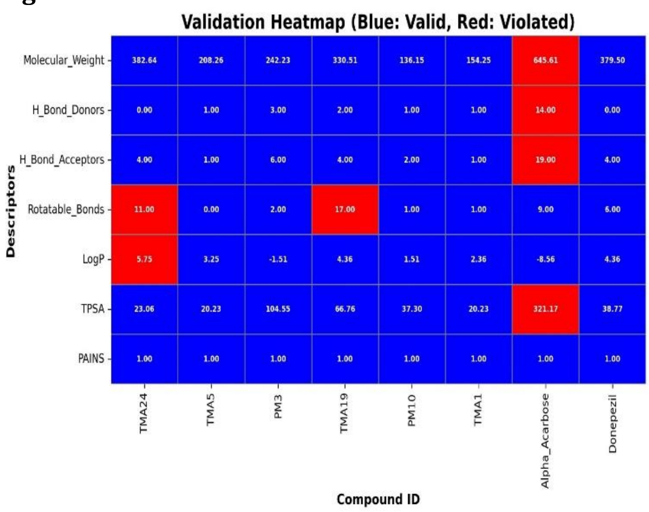

Figure shows the validation heatmap of test ligands and reference compounds (Donepezil and α-acarbose) based on key drug-likeness descriptors, where blue indicates compliance and red indicates violation. Most compounds satisfy molecular weight, H-bond donors/acceptors, TPSA, and PAINS filters. Violations are observed in LogP (TMA24), rotatable bonds (TMA24, TMA19), and TPSA (α-acarbose), while α-acarbose also exceeds limits in molecular weight and hydrogen bonding parameters. Overall, most test ligands, particularly TMA5, PM3, PM10, and TMA1, conform well to drug-likeness criteria, suggesting good pharmacokinetic potential compared to the reference standards.

ADMET Prediction

Comparative pharmacokinetic predictions of the phytochemicals and the reference drugs- donepezil and α-acarbose indicated the significant difference in absorption, distribution, metabolism, and safety. The α-acarbose (-

1.97) and PM10 (-0.847) exhibited high solubility and were preferentially absorbed orally, while donepezil (-4.648) and TMA24 (-7.132) exhibited low solubility, which might limit their bioavailability. However, the permeability of Caco-2, a measure of intestinal absorption, was higher in most phytochemicals (PM10 = 1.721; TMA5 = 1.493) than in donepezil (1.273) and significantly higher than in α-acarbose (0.638), suggesting that phytochemicals were more easily transported across the membrane. Human intestinal absorption was high (>90) regularly on all phytochemicals except PM3 (60.747) and 0% on α-acarbose, suggesting its gut action was local. This demonstrates that the phytochemicals, in particular, TMA24 and TMA5 are more accessible to the systemic circulation compared to the α-acarbose and even better compared to donepezil (Table 1). Regarding P-glycoprotein interactions that affect drug efflux and CNS penetration, donepezil and α-acarbose are P-gp substrates which can limit the brain bioavailability of the compounds of interest. The binding advantage of TMA24 (non-P-gp substrate) over donepezil in CNS delivery was observed. This observation was further supported by distribution parameters whereby BBB permeability was much higher in TMA24 (0.841) and TMA1 (0.566) than in donepezil. Furthermore, donepezil had few CYP3A4 substrates; thus, hepatically metabolized and there is a risk of drug-drug interaction. However, most of the phytochemicals had minimal potential to interact with CYPs. The variations in clearance values were moderate for donepezil (0.987 mL/min/kg) compared to TMA19 (1.975). These variations influence the safety profiles and the dose frequency in comparison with the reference drugs (Table 2). Donepezil exhibited hepatotoxicity, hERG II and hERG II inhibition. PM3 was predicted to be hepatotoxic, whereas TMA24 and TMA5 were not hERG I-inhibitory with an intermediate cardiac risk profile like that of donepezil. Phytochemicals such as TMA24 (1.298) had better systemic tolerance and maximum tolerated dose, in comparison to donepezil (-0.217) (Table 1).

Overall, the phytochemicals such as TMA24 and TMA1 demonstrated multiple key advantages over donepezil: better than BBB permeability, intestinal absorption, and less hepatotoxic, and comparable to alpha-acarbose in its systemic exposure and CNS penetration. The phytochemicals were predicted to have all much more appealing than α-acarbose in CNS availability and hence preferable agents in the treatment of selected diseases. TMA24 predicted to be an excellent candidate compared to donepezil because of high BBB penetration and low estimated hepatotoxicity, yet low solubility and enzyme selectivity profile need to be optimized.

Table 1 Table summarizes the pharmacokinetics and toxicity profiles of phytochemical ligands (TMA24, TMA5, PM3, TMA19, PM10, TMA1). It covers absorption (solubility, permeability, P-gp interaction), distribution (VDss, BBB and CNS permeability), metabolism (CYP enzyme interactions), excretion (total clearance), and toxicity (AMES test, LD50, hepatotoxicity, skin sensitization). These properties indicate their drug-likeness and safety potential for further development.

Table 1

Pharmacokinetic Properties		Phytochemical						Control	
Properties	**Model Name**	**TMA24**	**TMA5**	**PM3**	**TMA19**	**PM10**	**TMA1**	**Donepezil**	**α-acarbose**
Absorption	Water solubility	-7.132	-3.784	-2.369	-5.383	-0.847	-2.22	-4.648	-1.97
	Caco2 permeability	1.091	1.493	-0.109	0.439	1.721	1.496	1.273	-0.638
	Intestinal absorption (human)	91.053	96.064	60.747	90.922	93.307	93.625	93.707	0
	Skin Permeability	-2.482	-2.327	-2.949	-2.818	-2.192	-2.202	-2.585	-2.735
	P-glycoprotein substrate	No	Yes	No	No	No	Yes	Yes	Yes
	P-glycoprotein I inhibitor	Yes	No	No	Yes	No	No	Yes	No
	P-glycoprotein II inhibitor	Yes	No	No	No	No	No	Yes	No
Distribution	VDss (human)	0.772	0.738	-0.126	-0.25	0.131	0.196	1.266	-0.743
	Fraction unbound (human)	0	0.122	0.782	0.169	0.492	0.527	0	0.422
	BBB permeability	0.841	0.647	-0.896	-0.827	-0.222	0.566	0.157	-2.615
	CNS permeability	-1.363	-1.636	-3.58	-3.349	-2.076	-2.443	-1.464	-8.182
Metabolism	CYP2D6 substrate	Yes	No	No	No	No	No	Yes	No
	CYP3A4 substrate	Yes	Yes	No	Yes	No	No	Yes	No
	CYP1A2 inhibitor	Yes	Yes	No	Yes	No	No	No	No
	CYP2C19 inhibitor	Yes	Yes	No	No	No	No	No	No
	CYP2C9 inhibitor	No	No	No	No	No	No	No	No
	CYP2D6 inhibitor	No	Yes	No	No	No	No	Yes	No
	CYP3A4 inhibitor	No	No	No	No	No	No	Yes	No
Excretion	Total Clearance	0.319	0.021	0.689	1.975	0.148	0.173	0.987	0.478
	Renal OCT2 substrate	No	No	No	No	No	No	Yes	No
Toxicity	AMES toxicity	No	Yes	No	No	No	No	No	No
	Max. tolerated dose (human)	1.298	0.33	1.079	0.349	0.499	0.797	-0.217	0.469
	hERG I inhibitor	No	No	No	No	No	No	No	No
	hERG II inhibitor	yes	No	No	No	No	No	Yes	Yes
	Oral Rat Acute Toxicity (LD50)	2.45	2.176	2.054	1.708	2.086	1.756	2.753	2.386
	Oral Rat Chronic Toxicity (LOAEL)	1.785	1.225	2.762	2.747	2.071	1.938	0.991	7.486
	Hepatotoxicity	No	No	Yes	No	No	No	Yes	No
	Skin Sensitization	No	yes	No	Yes	Yes	Yes	No	No

Conclusion and Future Recommendations

This comparative in-silico study showed that phytochemicals have a potential as dual-targets for AChE and alpha-glucosidase. TMA24 exhibited the best interactions with AChE over donepezil and the TMA1 and PM3 were competitive with alpha-glucosidase compared with alpha-acarbose. Pharmacokinetics profiling of TMA24 and TMA1 indicated high intestinal absorption, and BBB permeability and the increased CNS uptake, in comparison with those of the reference drugs. Although the safety predictions indicated low hepatotoxicity and a reduced likelihood of enzyme inhibition for most phytochemicals, the observed hERG-II inhibition and mutagenic potential of certain compounds are noteworthy and warrant further investigation. Future approaches need to be involved in-vitro and in-vivo confirmation, optimization of solubility issues, minimization of cardiac risk of hERG II, and study of CYP-mediated warrants for applicability of top scored phytochemicals in clinical settings.

Authors' contribution

All authors have read and approved the manuscript. The author contributions are

Muhammad Junaid Yousaf: supervised the research and wrote the manuscript.

Mustafa Kamal and Basit Ali: conducted the original research.

Mughira Bin Zubair, Anwar Hussain and Naveed Ali: conducted statistical analysis and validated the data.

Acknowledgements

The authors extend their deep appreciation to Government Post Graduate College, Mardan for providing research facilities.

Ethical approval and consent to participate: Not applicable

Consent for publication: Not applicable

Data Availability: The data that support the findings of this study are available in the manuscript..

REFERENCES

1. Adnyaswari, D. A. M., et al. (2024). "*In silico* toxicity and pharmaceutical properties to get candidates for antitumor drug." Journal of Pharmaceutical Research International 36(2): 1-11. https://doi.org/10.9734/jpri/2024/v36i27497
2. Agarwal, U., et al. (2025). "A comprehensive review of supernatural coriander herb (Coriandrum sativum): phytochemical insights, pharmacological potential and future perspective." Phytochemistry Reviews: 1-47. https://doi.org/10.1007/s11101-025-10142-5
3. Agnihotry, S., et al. (2022). Protein structure prediction. Bioinformatics, Elsevier: 177-188. https://doi.org/10.1016/b978-0-323-89775-4.00023-7
4. Akshaya, R., et al. (2025). "Review on the Evolving Landscape of Molecular Docking in Drug Discovery." Asian Journal of Research in Pharmaceutical Sciences 15(3): 275-286. https://doi.org/10.52711/2231-5659.2025.00041
5. Andze, L., et al. (2024). "Innovative approach to enhance bioavailability of birch bark extracts: novel method of oleogel development contrasted with other dispersed systems." Plants 13(1): 145. https://doi.org/10.3390/plants13010145
6. Ansari, P., et al. (2025). "Therapeutic potential of medicinal plants and their phytoconstituents in diabetes, cancer, infections, cardiovascular diseases, inflammation and Gastrointestinal disorders." Biomedicines 13(2): 454. https://doi.org/10.3390/biomedicines13020454
7. Ayres, L. B., et al. (2024). "eutXG: A Machine-Learning Model to Understand and Predict the Melting Point of Novel X-Bonded Deep Eutectic Solvents." ACS Sustainable Chemistry & Engineering 12(30): 11260-11273. https://doi.org/10.1021/acssuschemeng.4c02844
8. Ayua, E. O., et al. (2021). "Polyphenolic inhibition of enterocytic starch digestion enzymes and glucose transporters for managing type 2 diabetes may be reduced in food systems." Heliyon 7(2). https://doi.org/10.1016/j.heliyon.2021.e06245
9. Barakat, H., et al. (2022). "Phenolics and volatile compounds of fennel (Foeniculum vulgare) seeds and their sprouts prevent oxidative DNA damage and ameliorates CCl4-induced hepatotoxicity and oxidative stress in rats." Antioxidants 11(12): 2318. https://doi.org/10.3390/antiox11122318
10. Bathula, R., et al. (2021). "Glide docking, autodock, binding free energy and drug-likeness studies for prediction of potential inhibitors of cyclin-dependent kinase 14 protein in wnt signaling pathway." Biointerface Res Appl Chem 12(2): 2473-2488. https://doi.org/10.33263/briac122.24732488
11. Bharath, N. (2023). Development of Process Technology for Production of Instant Mulberry Leaf Extract Powder, University of Agricultural Sciences, GKVK, Bangalore.
12. Bhatti, M. Z., et al. (2022). Plant secondary metabolites: therapeutic potential and pharmacological properties. Secondary metabolites-trends and reviews, IntechOpen. https://doi.org/10.5772/intechopen.103698
13. Bhujle, R. R., et al. (2025). "A comprehensive review on influence of millet processing on carbohydrate-digesting enzyme inhibitors and implications for diabetes management." Critical Reviews in Biotechnology 45(4): 743-765.
14. Chanu, M. B., et al. (2024). "GC-MS profiling, sub-acute toxicity study and total phenolic and flavonoid content analysis of methanolic leaf extract of Schima wallichii (DC) Korth-a traditional antidiabetic medicinal plant." Journal of Ethnopharmacology 330: 118111. https://doi.org/10.1016/j.jep.2024.118111
15. Dar, R. A., et al. (2023). "Exploring the diverse bioactive compounds from medicinal plants: a review." J. Phytopharm 12(3): 189-195.
16. Elbatawy, R. M., et al. (2025). "Comparative Study of the Antidiabetic and Hepatoprotective Effects of Coriander Seed Extract and Garlic Extract in an experimental Diabetic Rat Model." Egyptian Journal of Veterinary Sciences 56(13): 175-188. https://doi.org/10.21608/ejvs.2025.365881.2679
17. Endris, Y. A., et al. (2024). "Investigation of bioactive phytochemical compounds of the Ethiopian medicinal plant using GC-MS and FTIR." Heliyon 10(15).
18. Gaohua, L., et al. (2021). "Crosstalk of physiological pH and chemical pKa under the umbrella of physiologically based pharmacokinetic modeling of drug absorption, distribution, metabolism, excretion, and toxicity." Expert opinion on drug metabolism & toxicology 17(9): 1103-1124. https://doi.org/10.1080/17425255.2021.1951223
19. Garg, A. P. (2023). "Health Benefits of Cumin in Foods: A." Journal ISSN 2766: 2276.
20. Goyal, S., et al. (2022). "Trachyspermum ammi: a review on traditional and modern pharmacological aspects." Biological Sciences 2(4): 324-337. https://doi.org/10.55006/biolsciences.2022.2401
21. Guedri Mkaddem, M., et al. (2022). "Variation of the chemical composition of essential oils and total phenols content in natural populations of Marrubium vulgare L." Plants 11(5): 612.
22. Gupta, P., et al. (2024). "The Healing Herbs Of Traditional Medicine: A Review Of The Phytochemical And Pharmacological Significance Of Mentha Piperita (Peppermint)." European Journal of Biomedical 11(11): 378-386.

23. Hudz, N., et al. (2023). "Mentha piperita: Essential oil and extracts, their biological activities, and perspectives on the development of new medicinal and cosmetic products." Molecules 28(21): 7444. https://doi.org/10.3390/molecules28217444
24. Kazemi, A., et al. (2025). "Peppermint and menthol: a review on their biochemistry, pharmacological activities, clinical applications, and safety considerations." Critical reviews in food science and nutrition 65(8): 1553-1578.
25. Lahlou, R. A., et al. (2025). "Antioxidant and Anticoccidial Effects of Natural Phytogenic Additives in Broiler Chickens: An In Vitro and In Vivo Evaluation." https://doi.org/10.20944/preprints202507.0774.v1
26. Li, H., et al. (2024). "Structure determination of difficult-to-crystallize organic molecules by co-crystallization of a phosphorylated macrocycle." Organic Chemistry Frontiers 11(22): 6358-6366.
27. Lohit, N., et al. (2024). "Description and *in silico* ADME studies of US-FDA approved drugs or drugs under clinical trial which violate the Lipinski's rule of 5." Letters in Drug Design & Discovery 21(8): 1334-1358. https://doi.org/10.2174/1570180820666230224112505
28. Marbán-González, A., et al. (2025). "Exploiting PubChem and other public databases for virtual screening in 2025: what are the latest trends?" Expert Opinion on Drug Discovery(just-accepted).
29. Mishra, S., et al. (2024). "Microbial Degradation of Polyester Microfibers Using Indigenously Isolated Bacterial Strain Exiguobacterium Sp." CLEAN–Soil, Air, Water 52(12): e202300343. https://doi.org/10.1002/clen.202300343
30. Mitra, R., et al. (2025). "Identification of new small molecule allosteric SHP2 inhibitor through pharmacophore-based virtual screening, molecular docking, molecular dynamics simulation studies, synthesis and in vitro evaluation." Journal of Biomolecular Structure and Dynamics 43(3): 1352-1371.
31. Möbitz, H. (2024). "Design principles for balancing lipophilicity and permeability in beyond rule of 5 space." ChemMedChem 19(5): e202300395. https://doi.org/10.1002/cmdc.202300395
32. Modareskia, M., et al. (2022). "Thymol screening, phenolic contents, antioxidant and antibacterial activities of Iranian populations of Trachyspermum ammi (L.) Sprague (Apiaceae)." Scientific Reports 12(1): 15645.
33. Mohd Zaid, N. A., et al. (2023). "Promising natural products in new drug design, development, and therapy for skin disorders: An overview of scientific evidence and understanding their mechanism of action." Drug design, development and therapy: 23-66. https://doi.org/10.2147/dddt.s326332
34. Mołdoch, J., et al. (2025). "Biological activity of monoterpene-based scaffolds: A natural toolbox for drug discovery." Molecules 30(7): 1480.
35. Mughal, S. S. (2022). "A review on potential antioxidant effects of Cumin (Cuminum cyminum), phytochemical Profile and its uses." Authorea Preprints. https://doi.org/10.22541/au.166401164.45578619/v1
36. Najmi, A., et al. (2022). "Modern approaches in the discovery and development of plant-based natural products and their analogues as potential therapeutic agents." Molecules 27(2): 349.
37. Nhlapho, S., et al. (2024). "Druggability of pharmaceutical compounds using Lipinski rules with machine learning." Sciences of Pharmacy 3(4): 177-192. https://doi.org/10.58920/sciphar0304264
38. Ogbuagu, O. O., et al. (2022). "Novel phytochemicals in traditional medicine: Isolation and pharmacological profiling of bioactive compounds." International Journal of Medical and All Body Health Research 3(1): 63-71. https://doi.org/10.54660/ijmbhr.2022.3.1.63-71
39. Owoloye, A. J., et al. (2022). "Molecular docking, simulation and binding free energy analysis of small molecules as Pf HT1 inhibitors." PloS one 17(8): e0268269.
40. Riyaphan, J., et al. (2021). "*In silico* approaches to identify polyphenol compounds as α-glucosidase and α-amylase inhibitors against type-II diabetes." Biomolecules 11(12): 1877. https://doi.org/10.3390/biom11121877
41. Roba, B. B. and A. B. Umar (2025). "Investigating the potential of novel antioxidant flavonoids: a comprehensive study of drug-likeness, molecular docking, pharmacokinetics, and DFT analysis." Future Journal of Pharmaceutical Sciences 11(1): 1-17.
42. Roy, S., et al. (2024). "17 Molecular Docking and Molecular Dynamics in Signal Analysis." Signal Analysis in Pharmacovigilance: Principles and Processes: 210. https://doi.org/10.1201/9781032629940-17
43. Rudrapal, M., et al. (2024). "Dietary polyphenols: review on chemistry/sources, bioavailability/metabolism, antioxidant effects, and their role in disease management." Antioxidants 13(4): 429.
44. Singh, N., et al. (2021). "A review on traditional uses, phytochemistry, pharmacology, and clinical research of dietary spice Cuminum cyminum L." Phytotherapy Research 35(9): 5007-5030. https://doi.org/10.1002/ptr.7133
45. Studer, G., et al. (2021). "ProMod3—A versatile homology modelling toolbox." PLoS computational biology 17(1): e1008667.
46. Subramaniam, S., et al. (2021). "Cholinergic deep brain stimulation for memory and cognitive disorders." Journal of Alzheimer's Disease 83(2): 491-503. https://doi.org/10.3233/jad-210425
47. Suha, H. N., et al. (2025). "*In silico* discovery and predictive modeling of novel acetylcholinesterase (AChE) inhibitors for Alzheimer's treatment." Medicinal Chemistry 21(5): 345-366.
48. Tatarczak-Michalewska, M. and J. Flieger (2022). "Application of high-performance liquid chromatography with diode array detection to simultaneous analysis of reference antioxidants and 1, 1-diphenyl-2-picrylhydrazyl (DPPH) in free radical scavenging test." International journal of environmental research and public health 19(14): 8288. https://doi.org/10.3390/ijerph19148288
49. Thakur, G. S., et al. (2025). "Designing novel cabozantinib analogues as p-glycoprotein inhibitors to target cancer cell resistance using molecular docking study, ADMET screening, bioisosteric approach, and molecular dynamics simulations." Frontiers in Chemistry 13: 1543075.
50. Trivedi, T. S., et al. (2024). "Genome-wide characterization of fennel (Anethum foeniculum) MiRNome and identification of its potential targets in Homo sapiens and Arabidopsis thaliana: an inter and intra-species computational scrutiny." Biochemical Genetics 62(4): 2766-2795. https://doi.org/10.1007/s10528-023-10575-7
51. Ullah, M. A., et al. (2024). "Medical Constituents of Ajwain (Trachyspermum ammi) for Human Benefits." J General Med Clinical Practice.
52. Xie, W., et al. (2022). "Advances and challenges in de novo drug design using three-dimensional deep generative models." Journal of Chemical information and Modeling 62(10): 2269-2279.
53. Yadav, U., et al. (2022). Bioactive compounds in fennel seed. Spice Bioactive Compounds, CRC Press: 315-338. https://doi.org/10.1201/9781003215387-15

54. Zafar, S., et al. (2023). Fennel. Essentials of Medicinal and Aromatic Crops, Springer: 483-514. https://doi.org/10.1007/978-3-031-35403-8_19
55. Zeeshan, A., et al. (2023). "The healing touch of Foeniculum vulgare Mill.(Fennel): A review on its medicinal value and health benefits." Journal of Health and Rehabilitation Research 3(2): 793-800. https://doi.org/10.61919/jhrr.v3i2.226
56. Zhang, X., et al. (2022). "*In silico* methods for identification of potential therapeutic targets." Interdisciplinary Sciences: Computational Life Sciences 14(2): 285-310. https://doi.org/10.1007/s12539-021-00491-y
57. Zhang, Y., et al. (2023). "Benchmarking refined and unrefined AlphaFold2 structures for hit discovery." Journal of Chemical information and Modeling 63(6): 1656-1667. https://doi.org/10.1021/acs.jcim.2c01219.s001